

Determination of the Metabolites of FEONM, An Alzheimer's Disease Radio-Imaging Diagnosis Agent in Various Biosystems using LC/Tandem Mass Spectrometry

Wei-Hsi Chen^{1*}, Yu-Chieh Hsiao¹, Pei-Cheng Wang¹, Jenn-Tzong Chen², Kang-Wei Chang², Shiou-Shiow Farn², Wu-Jyh Lin² and Chyng-Yann Shiue^{3,4}

¹Chemistry Division, Institute of Nuclear Energy Research, Longtan District, Taoyuan City, Taiwan

²Isotope Application Division, Institute of Nuclear Energy Research, Longtan District, Taoyuan City, Taiwan

³PET Center, Department of Nuclear Medicine, National Taiwan University Hospital, Taipei, Taiwan

⁴PET Center, Department of Nuclear Medicine, Tri-Service General Hospital, Taipei, Taiwan

***Corresponding Author:** Wei-Hsi Chen, Chemistry Division, Institute of Nuclear Energy Research, Jiaan Village, Longtan District, Taoyuan City, Taiwan.

Received: July 07, 2017; **Published:** August 04, 2017

Abstract

The *in vitro* and *ex vivo* metabolites of FEONM (2-(1-{6-[(2-2-fluoroethoxyethyl)methylamino]-2-naphthyl}ethylidene)malononitrile) in various biosystems, such as liver microsomes, plasma, the liver and brain tissue homogenates, were determined using high-performance liquid chromatography coupled with electrospray ionization tandem mass spectrometry (HPLC/ESI-MS/MS). Positron-emitting isotope F-18 labeled FEONM (¹⁸F)FEONM) is an analogue of [¹⁸F]FDDNP, which has been used as a positron emission tomography (PET) imaging agent for diagnosing Alzheimer's disease. After solutions of FEONM were incubated with four biosystems respectively for specific durations, FEONM and its metabolites were separated from the biomatrices solutions using reversed-phase liquid chromatography (RP-LC), detected by diode array detector (DAD; $\lambda = 250$ nm), and analyzed by tandem mass spectrometry to determine their identities. Four, two, two, and two metabolites of FEONM were detected in the four biosystems: liver microsomes, plasma, the liver and brain tissue homogenates, in serially. The metabolism pathways of FEONM in the four biosystems were categorized to be demethylation, dealkylation of tertiary amine, oxidization and cleavage of dicyano-alkene into ketone group, hydrogenation of planar alkene, conjugation with glucuronic acid, and hydroxylation of ethoxy carbon. The former three reaction types had been reported previously for FDDNP but the later three ones have not been disclosed yet. The preliminary findings of the present study will provide information for using directions of PET imagination and the next works to examine FEONM and its metabolites distribution in the brain of living animal models by mass spectrometry imaging (MSI).

Keywords: Metabolism; FEONM; Alzheimer's Disease; PET Imaging Agent; HPLC/ESI-MS/MS

Introduction

Modern medicine has dramatically extended the lifetime of humans and as a result, the number of people older than sixty years has grown quickly worldwide. This has led to an increase in the number of aging diseases, such as Alzheimer's disease (AD) and other central nervous system disorders. Of these, AD is a common neurodegenerative disease accounting for 60-80% of all cases of dementia and is currently diagnosed using cognitive tests and mental state exams [1]. The primary neuropathology of AD includes cholinergic loss, extracellular deposition of amyloid- β plaques (A β plaque), formation of intracellular neurofibrillary tangles (NFT), chronic brain inflammation, oxidative damage and mitochondrial dysfunction [2]. Early diagnosis of AD pathogeny is difficult because of its complexity and current needs

Citation: Wei-Hsi Chen, *et al.* "Determination of the Metabolites of FEONM, An Alzheimer's Disease Radio-Imaging Diagnosis Agent in Various Biosystems using LC/Tandem Mass Spectrometry". *EC Pharmacology and Toxicology* 4.2 (2017): 40-50.

for specific imaging agents to detect diverse biomarkers. The ligand FEONM (2-(1-{6-[(2-2-fluoroethoxyethyl)methylamino]-2-naphthyl}thylidene)malononitrile, Figure 1) labeled with the positron radioisotope F-18 is an analogue of [¹⁸F]FDDNP (2-(1-{6-[(2-fluoroethyl)methylamino]-2-naphthyl}ethylidene)malononitrile) with fluoroethoxyethyl replaced for fluoroethyl [3]. [¹⁸F]FDDNP is known to have high lipophilicity (log P = 3.92) and is able to cross the blood-brain barrier (BBB) [4]. In addition, [¹⁸F]FDDNP was synthesized for positron emission tomography (PET) *in vivo* imaging for studying neurofibrillary deposits of hyperphosphorylated tau peptides (τ tangle) in the brain and low uptake of FDDNP in A β transgenic mice studies [5]. Both neurofibril pathological proteins are common biomarkers in AD patients and can be evaluated progressively [6-8]. PET image provides early *in vivo* detection of these neuropathological lesions that could provide visible evidence for evaluating future treatment strategies and outcomes for AD [8,9]. FEONM is more lipophilicity than FDDNP due to the additional alkyl group of fluoroethoxyethyl, which may allow FEONM to across the BBB more readily compared to FDDNP and is expected to be a potential new Tau protein PET imaging agent for early detection of AD [3].

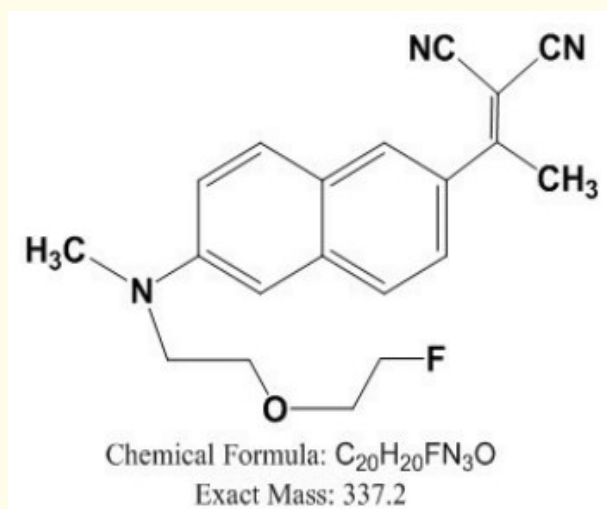


Figure 1: Molecular structure of FEONM.

Uptake and distribution profiles of ¹⁸F-FDDNP or ¹⁸F-FEONM in the body and organs could be imaged by PET. However, PET image is unable to differentiate the metabolites from parent ligands. The distribution of metabolites in the body and organs may also be different from the parent ligand, which might worsen the image resolution [10]. The metabolism of ¹⁸F-FDDNP by liver cytochrome P450 enzymes had been proposed to be two de-alkylation products of the tertiary-amine (demethylation and defluoroethylation, the non-radioactive metabolite) and one oxidized ketone product in addition to polar ethyl debris, such as F-18-labeled ethanol, ethanal, and acetic acid [4] which were derived from the study metabolism of ¹⁸F-FECNT (2 β -Carbomethoxy-3 β -(4-chlorophenyl)-8-(2-fluoroethyl)-nortropine, a PET agent for the dopamine transporter) ligand by high-performance liquid chromatography and mass spectrometric (HPLC-MS) techniques [10]. The xenobiotics were biotransformed to their metabolites mostly in the liver but they also occurred in other organs, such as the kidneys, small and large intestines, lungs, brain and so on to a lesser degree [11-13]. Despite the use of ¹⁸F-FEONM or ¹⁸F-FDDNP as imaging agents for the brain, neither compound nor metabolites have been well investigated. How fast is the ligand biotransformed into its metabolites, what are the metabolites and how do the ligand and metabolites distribute in the brain are the critical issues which need to be clarified for imaging biomarker patterns of AD patients.

As the brain is composed of various regions and accounting for different functions respectively, the PET ligand and its metabolites distribution might be different and impact on the image quality. On the other hand, the major approaches used to study metabolism pathways for xenobiotics are *in vitro* by cytosol, microsomes or hepatocytes, *ex vivo* (in the organ but out of the body) and *in vivo* of living animals [14]. It is more complicated and difficult to investigate *in vivo* metabolism. Therefore, the aim of the present study was to determine of the metabolites of FEONM *in vitro* (by rat liver microsomes) and *ex vivo* (by rodent liver, brain organ homogenate, and plasma respectively) using HPLC-electrospray ionization (ESI) triple quadrupole linear ion trap (QqQ LIT) tandem mass spectrometry (MS/MS). The results of LC-MS about identification of metabolites for FEONM in homogenous biosystems are the primary information for using directions of FEONM on PET imaging and in the next *in vivo* works, using matrix assisted laser desorption ionization (MALDI) coupled to time-of-flight (TOF) MS, namely mass spectrometry imaging (MSI) technique [15,16] to profile mapping of FEONM and its metabolites on the brain sections.

Materials and Methods

Materials and reagents

Analytical-grade chemicals for LC-MS were used. Methanol (HPLC- and MS-grade), dimethyl sulfoxide (DMSO), ammonium acetate, phosphate buffer pellets, sucrose and bovine serum albumin (BSA) were all purchased from Merck (Darmstadt, Germany). Ultrapure water was prepared using a reverse osmosis reagent water system (Smart DQ3, Merck Millipore, Billerica, MA, USA). FEONM (non F-18 labeled) was custom-synthesized by ABX GmbH (Radeberg, Germany) at a purity greater than 99%. Rat liver microsomes, coenzymes (NADPH) were purchased from BD Biosciences (Bedford, MA, USA) and stored at -70°C. Fresh rat liver was extracted from a healthy male Sprague-Dawley (SD) rat, and blood and mice brain were obtained from three healthy female mice (Balb/c) and pooled (Bio LASCOS Co., Taipei, Taiwan).

Analytical equipment

The biotransformation tendencies of FEONM in the liver microsomes, fresh liver and brain tissues homogenate, and plasma of rodents were surveyed by the component peak areas of HPLC chromatograms. HPLC system (Agilent 1100/1200 series, Palo Alto, CA, USA) with online degassed, binary pump, autosampler, and diode array detector (DAD) was used. Data were acquired and processed using the Agilent ChemStation software (ed. 10.02). The identities of metabolites were determined by MS/MS (4000 QTRAP®, AB Sciex, Concord, ON, Canada, with Analyst software 1.6.2) by analyzing mass-to-charge (m/z) ratio of molecular ions and fragments mass spectra.

Procedures of FEONM biotransformation

An FEONM standard was dissolved in DMSO (1 mg mL^{-1}) and took moderation [described in (a) and (b) sections] solution mixed with bioreaction systems for several time intervals (up to 4h) before quenching the bioreaction with the adding of methanol (1:1 volume), followed by mixing, centrifugation (6,000 rpm at 4°C for 10 min). The resultant supernatant was filtrated through $0.22\text{-}\mu\text{m}$ PVDF disk membrane and analyzed via HPLC-MS/MS.

- a) For rat liver microsome metabolites study: standard protocol of BD microsomes kit was followed and described here briefly. Microsomes (20 mg protein/mL) and NADPH coenzyme solution A and B were thawed using an ice bath. FEONM (3.3 mM , around 1000 ppm , $2 \mu\text{L}$) was mixed well with potassium phosphate buffer (0.5 M , $\text{pH } 7.4$), NADPH solution A and B, purified water, and the solution of microsomes ($25 \mu\text{L}$, i.e. 0.5 mg , added last) to total volume of $1000 \mu\text{L}$. Then, the tube was capped and placed in shaking water bath at 37°C for metabolism of FEONM to proceed.
- b) For rat liver and mouse brain tissue homogenates, and plasma metabolites studies: Normal rat liver and mice brain tissues were taken from a healthy male SD rats (32 weeks age) weighing 400g and three normal female mice (age: 6 weeks), respectively. The liver and brain tissues were freshly homogenized as described previously [17,18]. Rodents were sacrificed by CO_2 inhalation placing them in a closed box for 5 min until no vital signs could be observed. The whole liver (15g) and brain (1.4g) tissues were extracted, cleaned with cold saline solution, and immediately minced in a 0.25 M iced-cold sucrose solution. The liver and brain tissue solutions (40 and 5 mL , respectively, in tube) were mechanically homogenized (IKA T25 DS1, Germany) and transferred by whirling into 50- or 15-mL sample tubes. Blood (8 mL) was taken and pooled from the femoral artery of the three mice before sacrificed, immediately centrifuged to separate the corpuscles and the plasma; the volume of plasma obtained was around 4 mL . The homogenized tissues and plasma were stored at -70°C and used for *ex vivo* and *in vitro* metabolic studies freshly within 30 days. Tissues and plasma samples were used after thawed in iced bath. For the metabolism of FEONM studies, the tested solution composed of 0.25% BSA and 0.01 M phosphate buffer solution 1:1, 40 and $10 \mu\text{L}$ of FEONM stock DMSO solution were mixed with 2 and 0.5 mL of tissues homogenate (liver and brain), respectively. DMSO (40 or $10 \mu\text{L}$) without FEONM was mixed with the other agents solution under the same conditions to act as the controlled background. The plasma stability study for FEONM followed the assay protocol of Cyprotex [19]: mixing 0.4 mL of plasma with $4 \mu\text{L}$ of FEONM solution. All of the metabolism studied solutions of FEONM were placed in a shaking water bath at 37°C for specific durations.

Analytical method for biotransformation of FEONM

We used a C-18 reversed phase LC system (Eclipse XDB-C18, Agilent, with an inner diameter of 4.6 mm , length of 50 mm , and particle size at $1.8 \mu\text{m}$) with a programmed gradient mobile phase of aqueous ammonium acetate (10 mM) mixed with methanol. The mass spectrometry instrument consisted of an electrospray ionization (ESI) source, triple quadrupole linear ion trap (QQQ-LIT) mass detector, positive-ion detection mode, vaporized liquid nitrogen supplied for the sheath, auxiliary, curtain and collision gases. The coupled instrument parameters for determination of FEONM and its metabolites were listed in table 1.

HPLC	
Stationary phase	Eclipse XDB-C18, 4.6 mm x 50 mm, 1.8 mm
Injection volume, μL	3
Detector	DAD at 250 nm
Mobile phase	A: 10 mM $\text{NH}_4\text{Ac}_{(\text{aq})}$ 90% / MeOH 10% B: 10 mM $\text{NH}_4\text{Ac}_{(\text{aq})}$ 20% / MeOH 80%
Gradient program	0 ~ 3 min 50% B, isocratic 3~12 min up to 100% B and held for 5 min 17~20 min down to 0% B and held for 3 min to wash out salt of biomatrices 23~25 min up to 50% B and held for 5 min to re-condition of column
Flow rate, mL min^{-1}	0.5
Mass spectrometry	
Source temperature ($^{\circ}\text{C}$)	400
Detector polarity	Positive ion
Scanning mass range	100 - 1000
Resolution, Q1 and Q3	Unit
Nebulizer gas (p.s.i.)	40
Curtain gas (p.s.i.)	10
Collision gas (p.s.i.)	Medium or High for EMS and EPI modes, respectively ^a
Ion spray voltage (V)	5000
Declustering potential (V)	40

Table 1: Analytical parameters of HPLC/ESI-MS/MS for the determination of FEONM and its metabolites in biomatrices.

^a: EMS- enhanced mass spectrometry; EPI- enhanced product ion

Results and Discussion

HPLC-MS/MS method development

An RP-HPLC method was developed to analyze FEONM and its metabolites in biomatrices. The DAD detection wavelength was set at 250 nm for the best signal-to-noise ratio and sensitivity because the absorption band of naphthalene chromophore is around 250 nm. The polarities of FDDNP or FEONM are low as a result of the naphthalene group [4], and hence, the C18 column resulted in efficient retention for LC analysis. The optimization of the chromatographic analytical method was accomplished using a gradient of aqueous ammonium acetate mixed with methanol to give FEONM a retention time (t_r) of 13.18 ± 0.1 min, a theoretical plates number (N) of 36800, tailing factor 0.79, and a limit of quantitation (LOQ) approximately 40 ng mL^{-1} (based on UV detection, chromatogram shown in figure 2). The m/z ratios of molecular and fragmented ions of FEONM were 338 and, 304, 293, 274, 260, 246, 214. The fragmentation patterns for FEONM were plotted in figure 3 on the basis of MS/MS spectra of FEONM. The chromatographic purity (based on chromatographic peak area ratio) of the standard material was 99.35%. The molecular ion m/z of the most abundance impurity ($t_r = 11.7$ min) was 324, 14 units less than that of FEONM, and with a fragment ion 260. Therefore, the major impurity was the secondary amine of FEONM with a lost methyl group and contained 0.1%. Therefore, the purity of FEONM and our HPLC-MS/MS analytical method were suitable to study biotransformation pathways of FEONM.

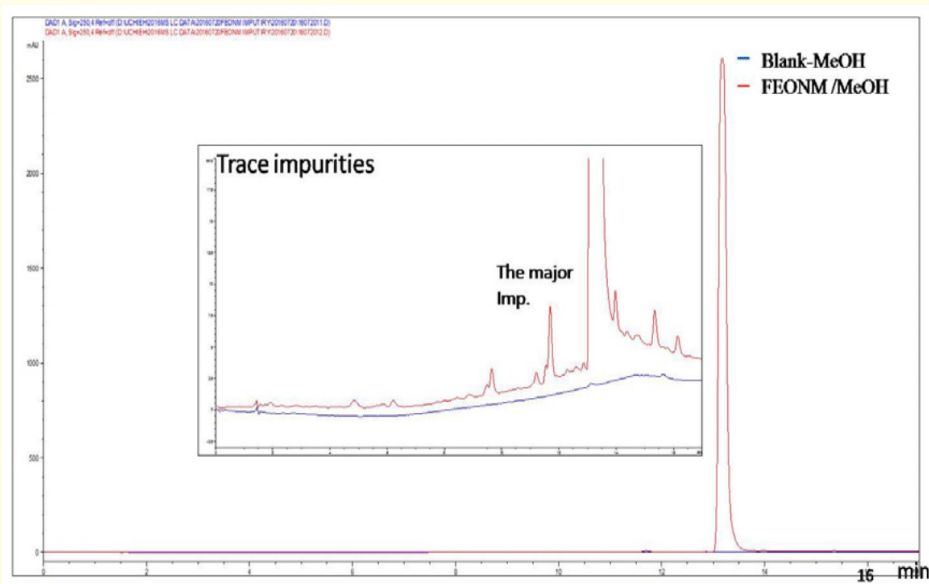


Figure 2: Chromatograms of FEONM standard material and its trace impurities.

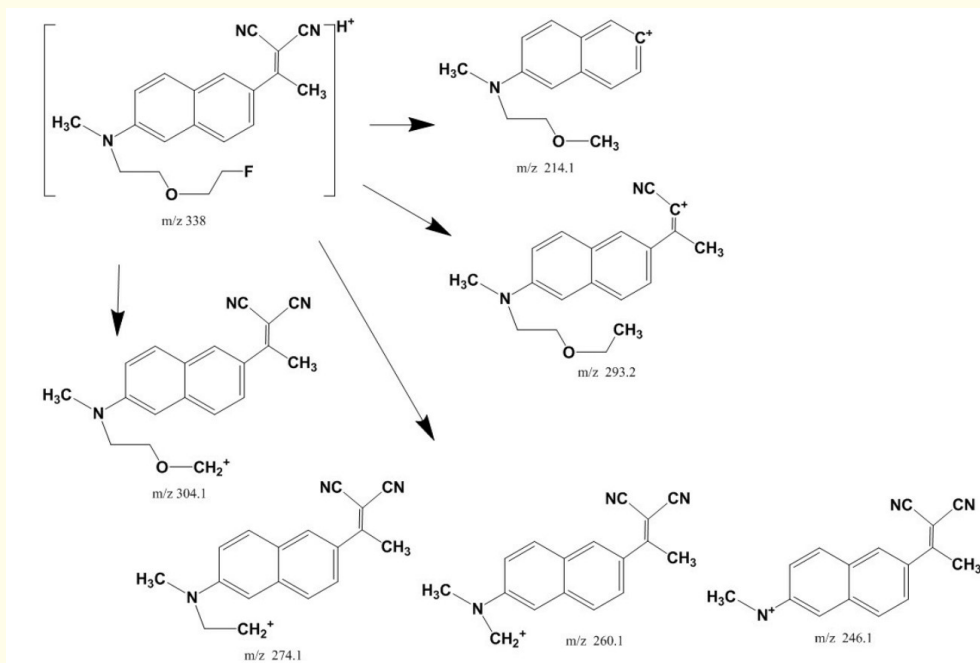


Figure 3: Proposed fragmentation patterns of FEONM based on MS/MS data.

In vitro study of FEONM metabolism using rat liver microsomes

In vitro metabolism of FEONM using commercial rat liver microsomes was examined first. The enzymatic system in liver microsomes composed of the CYP family catalyzing phase-I reactions [20]. As the reactions proceeded, the peak intensity and area of FEONM decreased and while the chromatographic peaks for four metabolites (M1 to M4) appeared; M4 was the most abundance product. Chromatographic retention times of M1 to M4 were 8.0, 9.5, 11.2, and 11.7 min, respectively. FEONM was readily metabolized: 25% of original FEONM remained after for 10 min reaction time and nearly exhausted after reaction for 60 min. On the other hand, the level of the major metabolites, M4, reached to the peak point at a reaction time of 10 min and then declined as it was metabolized to compounds M1 to M3. The chromatogram and levels tendencies for FEONM and its metabolites were shown in figure 4. To determine of the identities of M1 to M4, tandem mass spectra of the metabolites were examined. The m/z ratios of M4 molecular ion and its fragmented ions were 324 and 260, respectively, suggesting that the identity of M4 was also a contaminated impurity in FEONM parent ligand via de-methyl metabolized of tertiary amine. The tandem mass spectra data of M1 showed that M1 was a primary amine product resulting from dealkylation both methyl and fluoroethoxyethyl groups because of molecular and fragmented ions of M1 were 234, 217 ($\Delta M = -17$ than M1: $-NH_3$) and 155. So, it could not imagine in PET graph. There was a byproduct with an m/z ratio of 123 ($t_R = 2.08$ min based on MS detector); this could be interpreted that the cleaved fluoroethoxyethyl group was oxidized to fluoroethoxyacetic acid and preserved fluorine (imaginable). The byproduct is relative hydrophilic and can be easily cleared via urine; this might result in noise signal for PET all around the body. For the metabolite M2, m/z ratios for molecular and fragmented ions were 276, 234, 212 and 170. It was believed that M2 was the product of demethylation of amine and dicyano-alkene (deficient of electron) group degradation into ketone group (4). For M3, the molecular ion was 292 and fragmented ions signal were 274 ($\Delta M = -18$ [$-H_2O$] than M3) and 250. According to molecular ion m/z and relationship to FEONM and M2, the probable identity of M3 was suggested to be a hydroxylation product of M2 ($\Delta m/z = +16, +0$). M3 was the further step metabolite of M2 through hydroxylation on ethoxy-carbon.

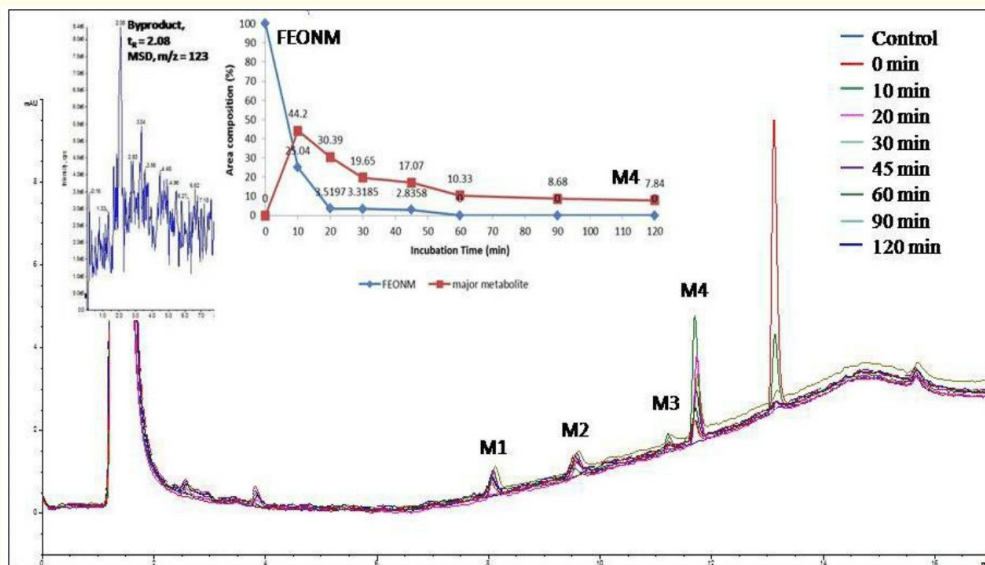


Figure 4: Chromatograms obtained from FEONM incubated in rat liver microsomes for various durations and peak levels over time for FEONM and its metabolites.

Ex vivo metabolism study of FEONM in the liver, brain and plasma

Ex vivo metabolism of FEONM using a rat liver homogenate was studied next. The fresh liver was homogenized immediately after extraction from the sacrificed rat. All enzymes of the liver were preserved in the reaction system to mimic *in vivo* conditions, in the meanwhile, all ligand and metabolites were well mixed and reacted with enzymes then contained in the reaction system without losing resulting from distribution all over the body [21]. After FEONM solutions were incubated for specific time durations (up to 240 min), levels of FEONM and its metabolites were monitored. The rate of metabolism of FEONM in rat liver homogenate was slower compared to that of rat liver microsomes and only two metabolites, major product M5 and minor M6, were produced with t_r of 11.7 and 12.1 min, respectively (Figure 5). The reaction tendency was mild until terminated it at 240 min, around 85% of FEONM remained. The m/z ratios of protonated M5 and its fragmented ions were 290 and 226, 184, 169. M5 was found to be like as M2 but it retained a methyl group ($\Delta M = +14$ of molecular and fragmented ions between M5 and M2, $+CH_3, -H$). And as a result, a tertiary amine and ketone derivative were formed. The m/z ratios of M6 and its fragmented ions were 340 ($\Delta M = +2$ than FEONM) and 276, respectively; therefore, M6 was inferred to be a hydrogenation ($+H_2$) product of FEONM; the alkene bond was hydrogenated to form saturated dicyano-isopropyl group with stereo hindrance as it was not coplanar with the naphthalene, moreover π electron delocalized structure of FEONM was destroyed.

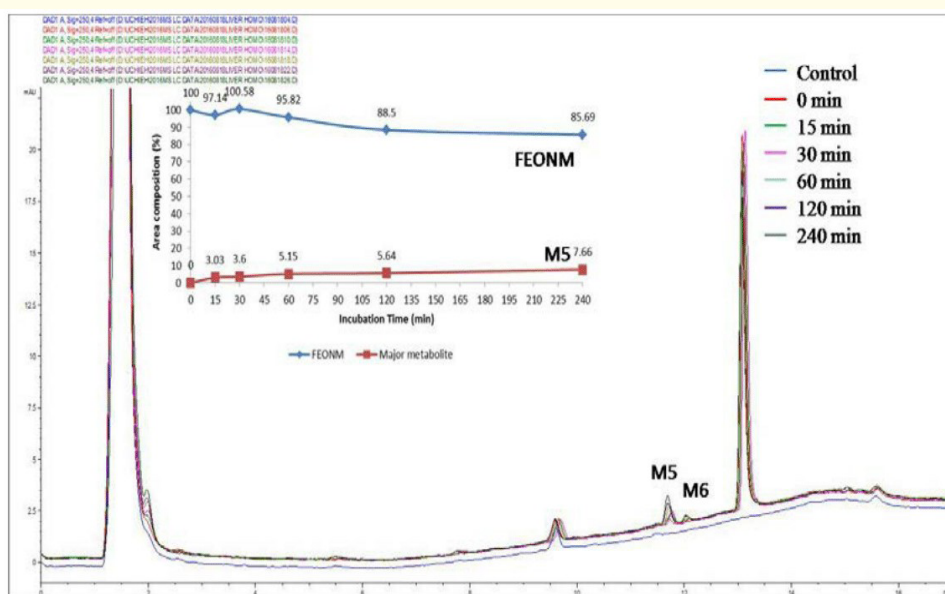


Figure 5: Chromatograms obtained from FEONM incubated in rat liver homogenate for various durations and peak levels over time for FEONM and its metabolites.

The brain was the target organ of FEONM imaged; hence, the resulting metabolites from enzymes in the brain might impact the quality of PET images. The metabolism study was performed using pooled healthy mice brain homogenate *ex vivo*. The rate of FEONM metabolized in the brain homogenate was obvious during the first 30 min but slow down afterward; at 240 min, approximately 54% as the original compound remained. The chromatogram (Figure 6) showed that there were two products, M7 and the major product M8 with t_r 11.7 and 12.1 min, respectively. The m/z ratios of M7 and its fragmented ions were 290, and 248, 226, 184, and 169, suggesting that M7 was chemically identical to M5, although it was not the major product. The m/z ratios for M8 and its fragmented ions were 340 ($\Delta m/z = +2$ than FEONM, $+2H$), and 276, 250, 211, and 184. The identity of M8 was believed to be identical to M6 found in the liver. Therefore, the metabolite M8 in the brain was excluded from the BBB due to its bulky dicyano-isopropyl group. It led to eliminate the ligand from the organ more easily.

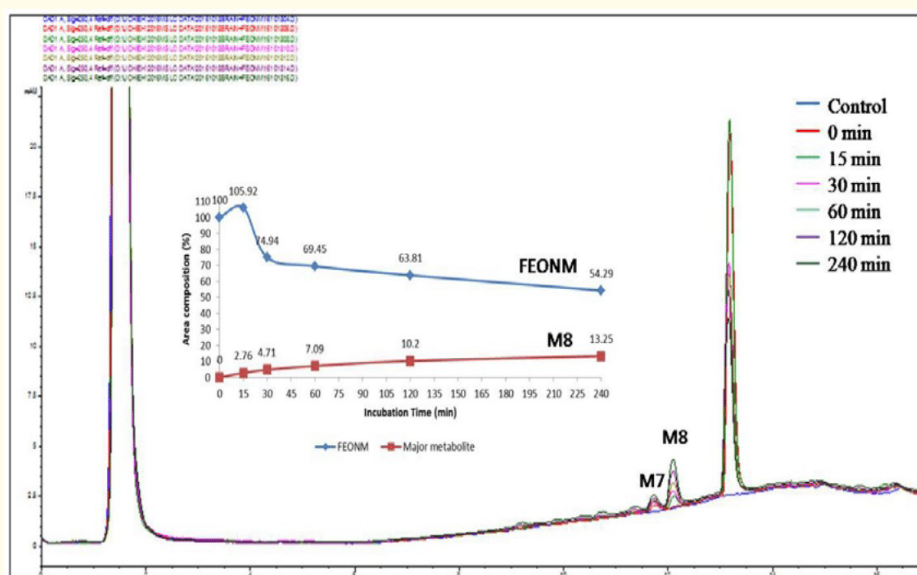


Figure 6: Chromatograms obtained from FEONM incubated in mice brain homogenate for various durations and peak levels over time for FEONM and its metabolites.

FEONM was intravenously administrated to animals to circulate through their whole bodies. FEONM was metabolized in plasma either before it arrived at or after it left from the organs. The plasma stability of FEONM supports its suitability for its original usage intention of PET imaging [22]. The level of FEONM was reduced to 58% of its original amount after a reaction of 60 min and further reduced to 12% after 4h. Two metabolites, major M9 ($t_R = 11.7$ min) and M10 ($t_R = 14.7$ min), were detected in the plasma matrix (Figure 7). The m/z ratios for M9 and its fragmented ions were 290, and 226, 184 and 169; these results inferred that M9 was the same molecule as M5, a metabolite from the rat liver homogenate study. The m/z ratios of M10 and its fragmented ions were 496, and 478, 184 and 104; these m/z ratios indicated that M10 was a conjugation product with glucuronidation (phase II metabolism).

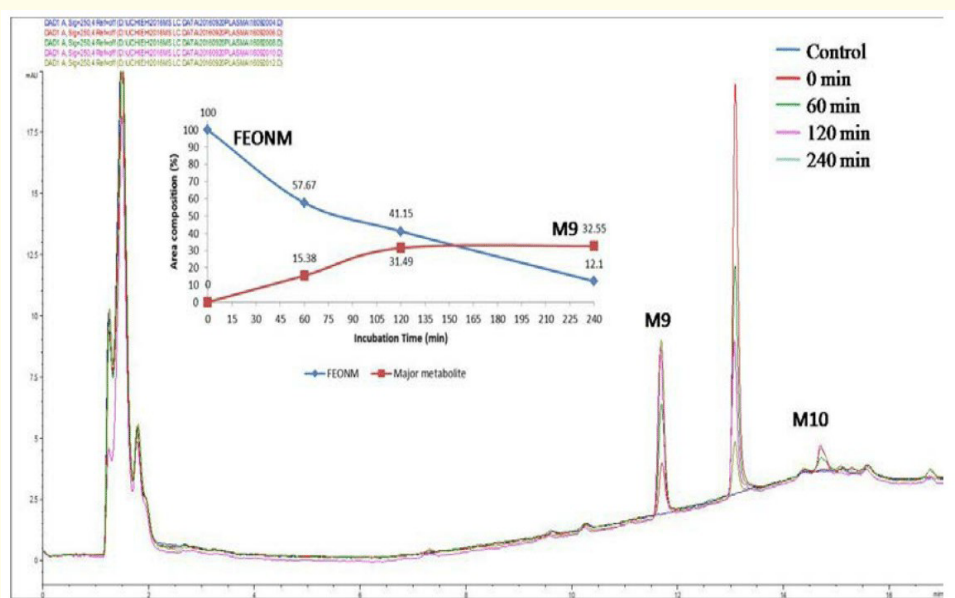


Figure 7: Chromatograms obtained from FEONM incubated in mice plasma for various durations and peak levels over time for FEONM and its metabolites.

Retention times, tandem mass spectra data and supposed major fragmented ions structured and identities of metabolites are summarized in Table 2. The metabolism pathways of FEONM in various bio-matrices are schematically represented in figure 8. To summarize, there were three susceptible functional groups present in the FEONM molecule that could be reacted upon to form its metabolites. Those were the methyl group, fluoroethoxyethyl at the tertiary amine and dicyano-alkene bond located beside the naphthalene group. The types of enzymatic reactions included demethylation, dealkylation of amine and oxidization, cleavage of dicyano-alkene into ketone group. Be-

cause cyano is a strong withdrawing electron group, dicyano-alkene was divided easily to be a ketone derivatives and formed M2, M3 and M5 (also M7, M9) metabolites. The byproduct of de-fluoroethoxyethyl from amino group formed its carboxylic acid: fluoroethoxy-acetic acid. It didn't collect m/z ratios less than 100 using the present method, hence smaller byproducts could not be detected. The found metabolites of FEONM in the present study were similar to those figured out by Luurtsema [4] for FDDNP metabolism pathways based on CYP450 enzymes but with various assemblies. Furthermore, two new metabolism pathways had not been disclosed previously until the study, which were hydrogenation on naphthalene co-planar alkene into a sterically bulky alkyl by the liver and brain tissues, and conjugation with glucuronic acid in plasma. Additionally, hydroxylation (adding OH group) on the ethoxy carbon by liver microsomes resulted in M3; this reaction was reported firstly because FDDNP does not contain an ethoxy group. All of the metabolites of FEONM in the four bio-systems are relieving its mission and lead to an enhanced rate of clearance from the brain and body.

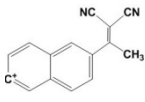
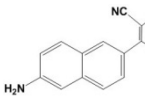
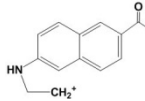
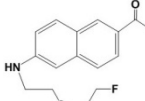
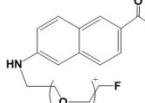
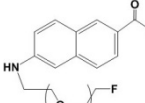
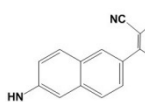
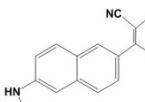
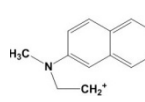
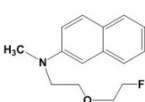
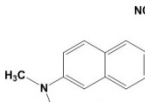
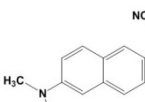
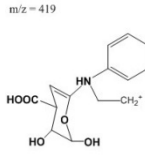
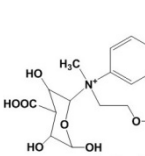
Biosystem	Metabolite#	t _R , min	m/z,	Supposed structure	
			Molecular ion;	Major fragmented ion	Metabolites
			Fragmented ions		
Rat liver microsomes	M1	8.0	234;		
			217, 199, 173, 155		
	Byproduct	2.1 (MSD)*	123;		FC ₂ H ₄ OCH ₂ COOH
	M2	9.5	276;		
			234, 212, 170		
	M3	11.2	292 (= M2 + 16);		
			274, 250		
	M4	11.7	324;		
			260		
Rat liver	M5	11.7	290;		
	M6	12.1	340 (= FEONM +2);		
			276, 211, 184		
Mice brain	M7	11.7	290;	As M5	
	M8	12.1	340 (= FEONM +2);	As M6	
			276, 211, 184		
Rat plasma	M9	11.7	290;	As M5	
	M10	14.7	496;		
			478, 419, 313, 283, 258, 184, 104		

Table 2: Retention time (t_R), tandem mass spectra data of metabolites in various biomatrices and their inferred identities.

*MSD: Mass spectrometry detector

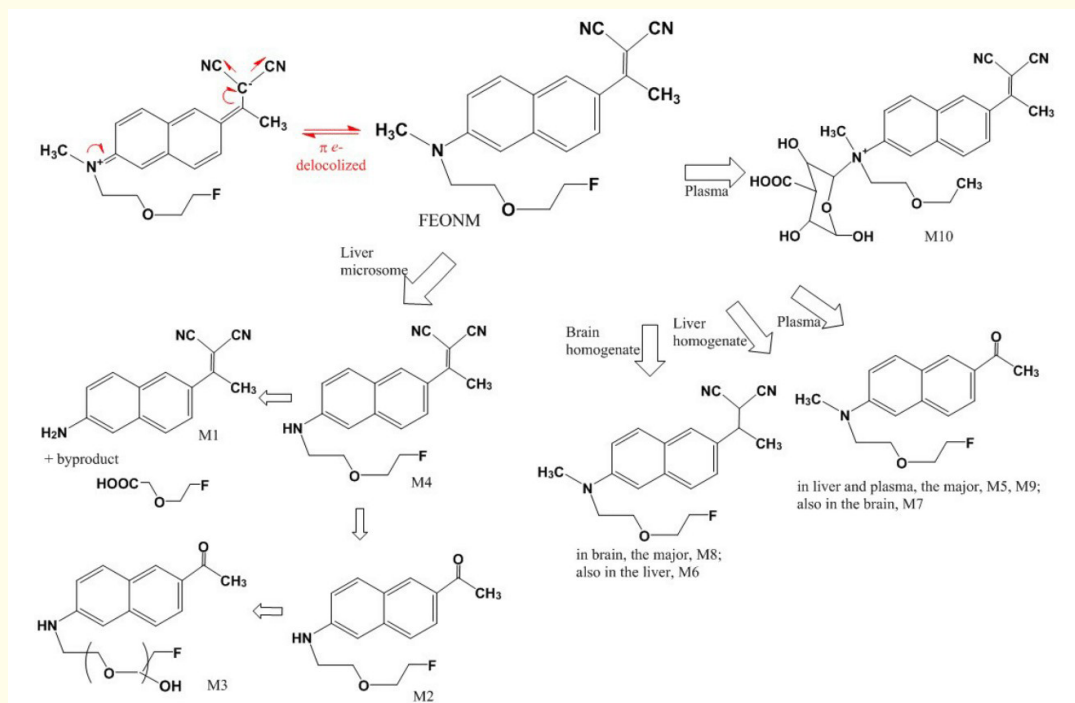


Figure 8: Scheme of the metabolites of FEONM metabolized by various biomatrices.

Conclusions

The results of the present investigation involve basic information that is necessary for the use of ^{18}F -FEONM as a PET imaging agent; this information provides the potential factors that might impact the images quality. As per the results it is suggested that PET images should be taken immediately after FEONM reaches its distribution equilibrium in the brain. It should be noted that the metabolism activities of the brain in an AD animal model may differ from those in healthy one, thereby resulting in differences. Therefore, future studies will focus on examining FEONM and its metabolites distribution using mass spectrometry imaging technique in living animal models.

Acknowledgements

The authors thank Chung-Long Lin and Zan-Chu Chen for preparation of the organs. The study was supported by a grant from the Atomic Energy Council, Taipei, Taiwan, R.O.C. (Grant No. 106-2001-02-10-01).

Bibliography

1. Pannee J. "Mass spectrometric quantification of amyloid-beta in cerebrospinal fluid and plasma-Implications for Alzheimer's disease" (2015).
2. Kumar A and Singh A. "New emerging trends in Alzheimer's disease drug research". *EC Pharmacology and Toxicology* 3.1 (2017): 15-17.
3. Hsu JP, et al. "Radiofluorination process development and Tau protein imaging studies of $[\text{F-18}]$ FEONM". *Journal of the Taiwan Institute of Chemical Engineers* 68 (2016): 119-129.

4. Luurtsema G., *et al.* "Peripheral metabolism of [18F]FDDNP and cerebral uptake of its labeled metabolites". *Nuclear Medicine and Biology* 35.8 (2008): 869-874.
5. Kuntner C., *et al.* "Limitations of small animal PET imaging with [18F]FDDNP and FDG for quantitative studies in a transgenic mouse model of Alzheimer's disease". *Molecular Imaging and Biology* 11.4 (2009): 236-240.
6. Liu J., *et al.* "High-yield, automated radiosynthesis of 2-(1-{6-[(2-[18F]fluoroethyl)(methyl)amino]-2-naphthyl}ethylidene) malononitrile ([18F]FDDNP) ready for animal or human administration". *Molecular Imaging and Biology* 9.1 (2007): 6-16.
7. Jovalekic A., *et al.* "New protein deposition tracers in the pipeline". *EJNMMI Radiopharmacy and Chemistry* 1 (2016): 11.
8. Yaqub M., *et al.* "Evaluation of tracer kinetic models for analysis of [18F]FDDNP studies". *Molecular Imaging and Biology* 11.5 (2009): 322-333.
9. Kepe V., *et al.* "Serotonin 1A receptors in the living brain Serotonin 1A receptors in the living brain of Alzheimer's disease patients". *Proceedings of the National Academy of Sciences of the United States of America* 103.3 (2006): 702-707.
10. Sami S Zoghbi., *et al.* "PET imaging of the dopamine transporter with 18F-FECNT: A polar radiometabolite confounds brain radioligand measurements". *Journal of Nuclear Medicine* 47.3 (2006): 520-527.
11. Xu N., *et al.* "Metabolism of cyadox by the intestinal mucosa microsomes and gut flora of swine, and identification of metabolites by high performance liquid chromatography combined with ion trap/time-of-flight mass spectrometry". *Rapid Communications in Mass Spectrometry* 25.16 (2011): 2333-2344.
12. Pai HV., *et al.* "Differential metabolism of Alprazolam by liver and brain cytochrome (P4503A) to pharmacologically active metabolite". *The Pharmacogenomics Journal* 2.4 (2002): 243-258.
13. Miksys S., *et al.* "Cytochrome P450-mediated drug metabolism in the brain". *Journal Psychiatry Neuroscience* 38.3 (2013): 152-163.
14. Brandon EFA., *et al.* "An update on in vitro test methods in human hepatic drug biotransformation research: pros and cons". *Toxicology and Applied Pharmacology* 189.3 (2003): 233-246.
15. Stoeckli, M., *et al.* "Compound and metabolite distribution measured by MALDI mass spectrometric imaging in whole-body tissue sections". *International Journal of Mass Spectrometry* 260.2-3 (2007): 195-202.
16. Reyzer ML and Caprioli RM. "MALDI-MS-based imaging of small molecules and proteins in tissues". *Current Opinion in Chemical Biology* 11.1 (2007): 29-35.
17. Marwah A., *et al.* "Ergosteroids VI. Metabolism of dehydroepiandrosterone by rat liver in vitro: a liquid chromatographic-mass spectrometric study". *Journal of Chromatography B: Analytical Technologies in the Biomedical and Life Sciences* 767.2 (2002): 285-299.
18. Chen WH., *et al.* "High performance liquid chromatography- tandem mass spectrometry method for ex vivo metabolic studies of a rhenium- labeled radiopharmaceutical for liver cancer". *European Journal of Mass Spectrometry* 20.5 (2014): 375-382.
19. Cyprotex Co. In vitro "ADME & PK - Plasma stability".
20. Patten C. "Human liver microsomes for *in vitro* drug metabolism studies". BD Biosciences Inc. Technical support (2009).
21. Hellman K., *et al.* "An *ex vivo* model for evaluating blood - brain barrier permeability, efflux, and drug metabolism". *ACS Chemical Neuroscience* 7.5 (2016): 668-680.
22. Wang G., *et al.* "High-throughput cassette assay for drug stability measurement in plasma using direct HPLC-MS/MS". *Spectroscopy* 17.2-3 (2003): 511-519.

Volume 4 Issue 2 August 2017

© All rights reserved by Wei-Hsi Chen., *et al.*